

# Capping with Multivalent Surfactants for Zeolite Nanocrystal Synthesis\*\*

Changbum Jo, Jinhwan Jung, Hye Sun Shin, Jaeheon Kim, and Ryong Ryoo\*

Nanoparticles have attracted a great deal of attention because they have a large accessible surface area and a remarkable difference in physicochemical properties when compared to bulk solids.<sup>[1]</sup> A versatile route to downsizing crystals to the nanoscale is to use an organic surfactant as a capping agent.<sup>[2]</sup> The surfactant prevents further crystal growth by covering nanoparticle surfaces by electrostatic attraction, coordination bonding, hydrogen bonding, or even using weak van der Waals interaction to the surface atoms. The surfactant-capping route is generally applied to the synthesis of various kinds of nanostructures, including nanoparticles and nanorods composed of metals, metal oxides, and chalcogenides.<sup>[3]</sup>

Zeolites are a family of microporous crystalline aluminosilicates consisting of more than 200 types of frameworks.<sup>[4]</sup> Currently, quite a few zeolites function as important ion-exchangers, molecular sieves, and catalysts.<sup>[5]</sup> Some zeolites are found as large mineral rocks in nature, but most zeolites used in the chemical industry are synthesized in the form of micrometer-sized crystallites. Despite the micrometer-scale size, the synthesized zeolite particles still contain more than  $10^9$  micropores. This characteristic can slow the rate of molecular diffusion through the microporous framework, often leading to limited catalytic performance.<sup>[6]</sup> To resolve the diffusive limitation, there have been numerous approaches focusing on the synthesis of nanocrystalline zeolites.<sup>[7]</sup> However, most approaches were limited to particular types of zeolites under special synthesis conditions<sup>[8]</sup> or were dependent on specially synthesized zeolite structure-directing agents (SDA).<sup>[9]</sup> Cetyltrimethylammonium bromide (CTABr) is well known for its mesopore-directing effect in the synthesis of mesoporous silicas.<sup>[10a]</sup> However, CTABr fails to function as a mesopore-directing agent when the surfactant was added to a zeolite synthesis composition in an attempt to synthesize mesoporous material with a crystalline zeolitic framework.<sup>[10b,c]</sup> There are a few reports on the synthesis of LTA (Linde type A) zeolite nanocrystals in the presence of CTABr by a low crystallization and growth rate technique.<sup>[10d-f]</sup> However, the surfactant capping was not so effective

as to justify a general application to the synthesis of other zeolites. We believe that the lack of effectiveness of zeolite capping was due to the presence of other cationic species, such as  $\text{Na}^+$  and zeolite structure-directing ammonium ions that could compete with  $\text{CTA}^+$  ions during the hydrothermal synthesis of zeolites.

Synthesis of nanocrystalline zeolites using multivalent surfactants (MSs) has been reported recently. For example, Ryoo and co-workers synthesized MFI, MRE, beta, and MTW zeolites in the form of nanosheets or nanosponges, using  $\text{C}_{22}\text{H}_{45}\text{N}^+(\text{Me})_2\text{C}_6\text{H}_{12}\text{N}^+(\text{Me})_2\text{C}_6\text{H}_{13}$  and other cationic surfactants containing three or more ammonium ions.<sup>[11]</sup> The role of the surfactants was to direct a mesostructure by forming a micelle while micropores were generated by individual surfactant head groups. Hensen and co-workers synthesized a mesoporous CHA zeolite by incorporating  $\text{C}_{22}\text{H}_{45}\text{N}^+(\text{Me})_2\text{C}_4\text{H}_8\text{N}^+(\text{Me})_2\text{C}_4\text{H}_9$  as a mesopore-generating agent into a synthesis composition containing *N,N,N*-trimethyl-1-adamantanammonium hydroxide for the micropore generation.<sup>[12]</sup> The mesopore generation was attributed to the effect of growth interruption of zeolite crystals. However, such an effect was not so far confirmed for other zeolites or other surfactants.

Herein, we show that various zeolite nanocrystals could readily be synthesized, such as MOR, FAU(X), CHA, and MFI types, when cationic MSs that contain two or more ammonium head groups were added to the hydrothermal synthesis compositions. The zeolite nanocrystals became agglomerated so that they possessed intercrystalline mesopores. We characterized the zeolite samples using scanning electron microscopy (SEM), transmission electron microscopy (TEM), X-ray diffraction (XRD), and  $\text{N}_2$  adsorption-desorption isotherms. Our results indicated that the MSs could protect zeolite nanocrystal surfaces from further growth more effectively than CTABr, which is probably due to strong electrostatic interactions. Because of their nanocrystal size, the MOR zeolites obtained by MS-capping exhibited high catalytic performance as solid acid catalysts for cumene synthesis reaction.

We tested  $\text{C}_{18}\text{H}_{37}\text{N}^+(\text{Me})_2\text{C}_6\text{H}_{12}\text{N}^+(\text{Me})_2\text{C}_6\text{H}_{12}\text{N}^+(\text{Me})_2\text{C}_{18}\text{H}_{37}$  (" $\text{C}_{18}\text{-N}_3\text{-C}_{18}$ " for brevity) as a surfactant for the capping of MOR zeolite nanocrystals. The surfactant was added to a conventional synthesis composition for a MOR zeolite. The synthesis temperature was 423 K (see the Experimental Section). The zeolite sample synthesized with  $\text{C}_{18}\text{-N}_3\text{-C}_{18}$  is denoted by MOR-nrod. On the other hand, a control sample synthesized without using  $\text{C}_{18}\text{-N}_3\text{-C}_{18}$  is denoted by MOR-bulk. The XRD pattern of MOR-nrod was consistent with the structure of the MOR-type zeolite (Supporting Information, Figure S1). As compared to

[\*] C. Jo, J. Jung, H. S. Shin, J. Kim, Prof. R. Ryoo  
Center for Nanomaterials and Chemical Reactions  
Institute for Basic Science (IBS)  
Daejeon 305-701 (Republic of Korea)  
and  
Department of Chemistry, KAIST  
Daejeon 305-701 (Republic of Korea)  
E-mail: rryoo@kaist.ac.kr  
Homepage: <http://rryoo.kaist.ac.kr>

[\*\*] This work was supported by the Institute for Basic Science in Korea.  
Supporting information for this article is available on the WWW under <http://dx.doi.org/10.1002/anie.201303088>.

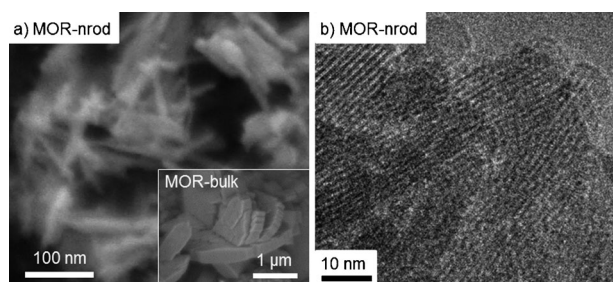


**Figure 1.** a) SEM image and b) TEM image of MOR nanorods, which were synthesized with a trivalent surfactant,  $C_{18}N_3-C_{18}$ . For comparison, SEM image of MOR-bulk is shown in the inset of (a).

MOR-bulk, MOR-nrod exhibited XRD line broadening. The estimation of crystal size using the Scherrer equation from (200) reflection gave 17 nm for the MOR-nrod zeolite. The SEM image for MOR-nrod (Figure 1a) exhibited agglomeration of nanorods with a flat cross section. Typical dimension of the nanorods ranged from 10 to 15 nm in width, 4 to 6 nm in thickness, and 100 to 300 nm in length, as judged from TEM imaging (Figure 1b; Supporting Information, Figure S1). The longest side of the nanorods is parallel to the *c*-axis of a MOR structure (Supporting Information, Figure S1). On the other hand, the MOR-bulk sample exhibited micrometer-sized crystal morphologies with 1–2 μm particle diameters (inset of Figure 1a). The *t*-plot method was used to determine the external crystal surface area of these zeolite samples. The external surface area for MOR-nrod obtained in this manner was 220 m<sup>2</sup> g<sup>−1</sup>, whereas MOR-bulk was only 5 m<sup>2</sup> g<sup>−1</sup> (Supporting Information, Figure S1). The difference in external surface areas was in good agreement with their particle size difference. Elemental analysis (EA) revealed that the freshly synthesized MOR-nrod sample (before calcination) contained organic components corresponding to 15% (*w/w*) of its total mass. Before the EA, the MOR-nrod sample was washed with ethanol and water to remove any organic components that might be weakly physisorbed. Therefore, the 15% (*w/w*) loss could be assigned to the  $C_{18}N_3-C_{18}$  surfactant. Since the  $C_{18}N_3-C_{18}$  molecule was too bulky to enter the micropore aperture of MOR zeolite, the amount of surfactant was believed to remain on the external surfaces through electrostatic interactions between the ammonium heads of the surfactants and the zeolite framework. The surfactant amount, based on the monolayer assumption, was consistent with the measured 15% loss (see the Supporting Information, Section S2 for a detailed calculation). Therefore, the generation of the nanocrystals could be attributed to the capping effect of  $C_{18}N_3-C_{18}$ . The surfactant capping was confirmed to work effectively until the concentration of the reaction gel was increased twice by decreasing the amount of water to a half as compared to the gel composition described in the Experimental Section. Below this water content, however, the nanocrystalline MOR zeolite product contained sodalite zeolite as an impurity phase.

The nanomorphologies of MOR zeolites could be controlled by the use of different capping surfactants. For example, MOR zeolite was synthesized in the form of nanosheet (MOR-nsht) when a divalent surfactant with the

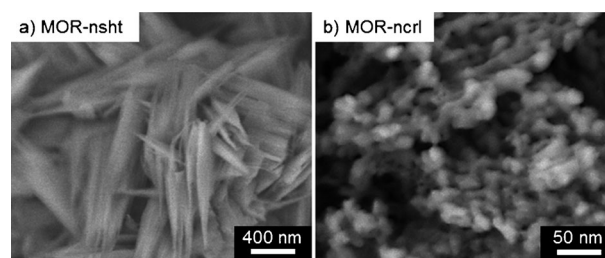


**Figure 2.** SEM images of MOR zeolite samples synthesized with multivalent capping surfactants: a) MOR nanosheets synthesized with a divalent surfactant; b) MOR nanocrystals synthesized with a prolinol derivative trivalent surfactant.

structural formula of  $C_{18}H_{37}N^+(Me)_2C_6H_{12}N^+(Me)_2C_{18}H_{37}$  was used as the capping agent (Figure 2a). When a prolinol derivative, trivalent surfactant  $C_{18}H_{37}N^+(Me)_2C_6H_{12}N^+(Me)_2CH_2C_6H_4CH_2N^+(Me)(C_4H_7CH_2OH)$  (see the Supporting Information, Figure S3 for the structure) was used, the morphology of the MOR zeolite was observed to be an aggregation of nanocrystals (MOR-ncrl in Figure 2b). The diameter of the individual MOR nanocrystals ranged from 10 to 30 nm, as determined by high-resolution TEM (Supporting Information, Figure S3). On the other hand, when the monovalent cationic surfactant  $C_{18}H_{37}N^+(Me)_2C_{18}H_{37}$ , or CTA<sup>+</sup>, was tested as a capping agent, the resultant product was very similar to MOR-bulk. From this result, we believe that the multiple charges are important for the capping effect of a cationic surfactant during zeolite synthesis. Certainly, the exclusive use of these surfactants does not make them MOR zeolite structure-directing agents.<sup>[11a,c]</sup>

The surfactant-capping route was further tested for FAU(X), MFI, and CHA zeolites using  $C_{18}N_3-C_{18}$ . All the resultant zeolites gave SEM images showing agglomerates of nanocrystals (Figure 3). On the other hand, when these zeolites were synthesized without  $C_{18}N_3-C_{18}$ , all the products were micrometer-sized crystals with smooth surfaces (Supporting Information, Figure S5). The crystal sizes were 20–

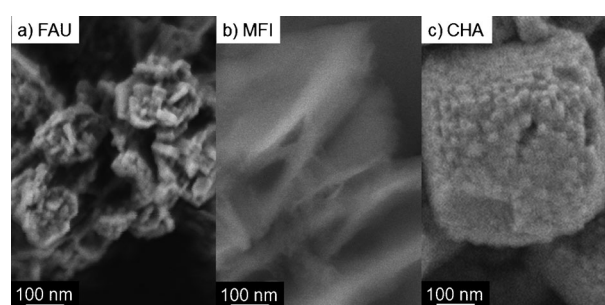


**Figure 3.** SEM images of a) FAU, b) MFI, and c) CHA zeolite nanoparticles, which were synthesized with  $C_{18}N_3-C_{18}$  as a capping agent.

40 nm in the case of the nanocrystalline FAU(X) zeolites (see the Supporting Information, Figure S4 for TEM). The external surface area was 118 m<sup>2</sup> g<sup>−1</sup>, and this was much higher than 2 m<sup>2</sup> g<sup>−1</sup> of the bulk counterpart. Similarly, crystal-capping effect of the trivalent surfactant was confirmed in MFI zeolite synthesis. The MFI zeolite synthesized with the

surfactant has the form of agglomerates of 10–20 nm thick nanosheets (Supporting Information, Figure S4). In the case of CHA zeolite, nanocrystalline (20–30 nm) CHA zeolite possessing intercrystalline mesopores was also obtained by the addition of  $C_{18}-N_3-C_{18}$  surfactant (Figure 3). This zeolite possessed intercrystalline mesopores amounting to  $0.2\text{ cm}^3\text{ g}^{-1}$ . However, the mesoporosity decreased gradually when the zeolite product was kept in the synthesis reaction mixture over a long period of several days after the initial nanocrystal formation. It thus seemed that the crystal capping effect decreased owing to Ostwald ripening.

The decrease in particle size to a nanometer dimension can be a remarkable benefit where zeolite catalysts suffer from diffusion limitations. For example, the MOR-nrod with a Si/Al ratio of 8.5 exhibited much higher activity and longer catalytic lifetime in the cumene synthesis reaction than showed by the MOR-bulk zeolite (Si/Al = 7). Cumene is a precursor for the synthesis of other industrially important chemicals, such as phenol and acetone. The conversion rates of the reactants were plotted (Supporting Information, Figure S6) as a function of time on stream to determine the lifetime of catalysts. MOR-nrod exhibited an initial activity of 85% and maintained this value even after 20 h. In contrast, MOR-bulk showed very low initial activity (20%) and rapidly deactivated. This high catalytic performance of MOR-nrod can be attributed to reactions occurring at the external surfaces,<sup>[11e]</sup> or the short diffusion path lengths in the mesoporous zeolite.<sup>[13]</sup> So far, no direct synthetic methods for the successful production of highly crystalline MOR nanocrystals less than 100 nm in size have been reported.<sup>[14]</sup> Organosilane surfactants and zeolite structure-directing surfactants were tested during the course of the present study, but the results have not yet indicated success. Post-synthetic demetalation treatments have been reported as an effective means of mesopore generation in MOR zeolites by Jong et al.<sup>[15]</sup> Mesoporous zeolites exhibited high catalytic activity in liquid phase cumene synthesis,<sup>[15]</sup> but the effect of the mesopores on catalytic lifetime was unknown.

In conclusion, the capping effect of the multivalent cationic surfactants allowed us to synthesize FAU, MOR, CHA, and MFI-type zeolite nanocrystals. The zeolite morphologies (nanoparticles, nanorods, and nanosheets) were still controlled in a passive manner by the surfactants, and they were probably also dependent on the zeolite structures. Nevertheless, the multivalent surfactant-capping route would be suitable for the synthesis of other zeolite nanocrystals that could improve existing catalytic applications and even enable new applications. The nanocrystal formation is attributed to the multiply and thereby strongly binding effect of the surfactant molecules on the substrate surfaces, as compared to monovalent surfactants. In principle, the multiple binding effects are similar to the synthesis of very stable gold nanoparticles using multi thiols.<sup>[16]</sup> Therefore, we believe that the multivalent surfactant capping could be generally applicable to various compositions of nanomaterials, such as metals, metal oxides, MOFs, and chalcogenides.

## Experimental Section

Detailed procedures for the synthesis of multivalent surfactants presented in this paper are described in the Supporting Information. MOR nanorods with  $C_{18}-N_3-C_{18}$  as a capping agent were synthesized as follows: Aluminum sulfate octadecahydrate ( $\geq 98\%$ , Sigma-Aldrich) and  $C_{18}-N_3-C_{18}$  was completely dissolved in distilled water. Into the clear solution, sodium silicate (Si/Na = 1.75, 29 wt %  $\text{SiO}_2$ , Shinheung Silicate Co., Ltd.) was added at once and the mixture was vigorously shaken by hand for 10 min. Then, sulfuric acid (47%, Wako) was dropped into the gel mixture. The resultant gel had a molar composition of 30:1.5:1.3:8.57:1200:4.5  $\text{SiO}_2/\text{Al}_2\text{O}_3/C_{18}-N_3-C_{18}/\text{Na}_2\text{O}/\text{H}_2\text{O}/\text{H}_2\text{SO}_4$ . After continuous mixing using a magnetic stirrer for 12 h at 298 K, the resultant gels were transferred into a Teflon-lined stainless steel autoclave. The autoclave tumbled at 60 rpm in an oven heated at 423 K. The sample was collected from a homogeneous gel solution at 8 days. All of the samples were dried at 373 K and calcined in air at 853 K. The production yield of MOR-nrod was more than 85%. The synthesis method of MOR zeolites synthesized by using  $C_{18}-N_1-C_{18}$ ,  $\text{CTA}^+$ ,  $C_{18}-N_2-C_{18}$ , and prolinol-containing surfactant as capping agents is the same as that of MOR nanocrystal synthesized by using  $C_{18}-N_3-C_{18}$ . The synthesis procedures of other zeolite nanocrystals are described in the Supporting Information.

Received: April 12, 2013

Revised: June 7, 2013

Published online: August 1, 2013

**Keywords:** capping agents · multivalent surfactants · nanoparticles · zeolites

- [1] a) R. B. Laughlin, *Phys. Rev. Lett.* **1983**, *50*, 1395; b) J. Hu, T. W. Odom, C. M. Lieber, *Acc. Chem. Res.* **1999**, *32*, 435; c) M. Law, J. Goldberger, P. Yang, *Annu. Rev. Mater. Res.* **2004**, *34*, 83; d) A. K. Geim, K. S. Novoselov, *Nat. Mater.* **2007**, *6*, 183.
- [2] a) A. L. Rogach, A. Kornowski, A. Eychmüller, H. Weller, *J. Phys. Chem. B* **1999**, *103*, 3065; b) S. Bhattacharya, A. Srivastava, A. Pal, *Angew. Chem.* **2006**, *118*, 3000; *Angew. Chem. Int. Ed.* **2006**, *45*, 2934; c) Y. Lu, X. Lu, B. T. Mayers, T. Herricks, Y. Xia, *J. Solid State Chem.* **2008**, *181*, 1530.
- [3] a) M. S. Bakshi, G. Kaur, P. Thakur, T. S. Banipal, F. Possmayer, N. O. Peterson, *J. Phys. Chem. C* **2007**, *111*, 5932; b) T. K. Sau, C. J. Murphy, *Langmuir* **2005**, *21*, 2923; c) T. Mokari, M. Zhang, P. Yang, *J. Am. Chem. Soc.* **2007**, *129*, 9864; d) J. Joo, H. B. Na, T. Yu, J. H. Yu, Y. W. Kim, F. Wu, J. A. Zhang, T. Hyeon, *J. Am. Chem. Soc.* **2003**, *125*, 11100.
- [4] a) M. E. Davis, R. F. Lobo, *Chem. Mater.* **1992**, *4*, 756; b) C. S. Cundy, P. A. Cox, *Chem. Rev.* **2003**, *103*, 663.
- [5] a) A. Corma, *Chem. Rev.* **1995**, *95*, 559; b) S. Aguado, G. Bergeret, C. Daniel, D. Farrusseng, *J. Am. Chem. Soc.* **2012**, *134*, 14635; c) K. Varoon, X. Y. Zhang, B. Elyassi, D. D. Brewer, M. Gettel, S. Kumar, J. A. Lee, S. Maheshwari, A. Mittal, C.-Y. Sung, M. Cococcioni, L. F. Francis, A. V. McCormick, K. A. Mkhoyan, M. Tsapatsis, *Science* **2011**, *334*, 72, see Supporting Information; d) J. Čejka, B. Wichterlová, *Catal. Rev.* **2002**, *44*, 375.
- [6] a) J. C. Groen, W. Zhu, S. Brouwer, S. J. Huynink, F. Kapteijn, J. A. Moulijn, J. Pérez-Ramírez, *J. Am. Chem. Soc.* **2007**, *129*, 355; b) O. C. Gobin, S. J. Reitmeyer, A. Jentys, J. A. Lercher, *J. Phys. Chem. C* **2009**, *113*, 20435; c) D. Theodorou, J. Wei, *J. Catal.* **1983**, *83*, 205.
- [7] a) D. P. Serrano, J. Aguado, J. M. Escola, J. M. Rodríguez, *J. Anal. Appl. Pyrolysis* **2005**, *74*, 353; b) G. Li, C. A. Jones, V. H. Grassian, S. C. Larsen, *J. Catal.* **2005**, *234*, 401; c) J. Kecht, S. Mintova, T. Bein, *Chem. Mater.* **2007**, *19*, 1203; d) W. J. Roth,

- O. V. Shvets, M. Shamzhy, P. Chlubná, P. Kubů, P. Nachtigall, J. Čejka, *J. Am. Chem. Soc.* **2011**, 133, 6130; e) W. C. Yoo, S. Kumar, R. L. Penn, M. Tsapatsis, A. Stein, *J. Am. Chem. Soc.* **2009**, 131, 12377.
- [8] a) W. Song, V. H. Grassian, S. C. Larsen, *Chem. Commun.* **2005**, 2951; b) K. Möller, B. Yilmaz, R. M. Jacubinas, U. Müller, T. Bein, *J. Am. Chem. Soc.* **2011**, 133, 524; c) H. Wang, B. A. Holmberg, Y. Yan, *J. Am. Chem. Soc.* **2003**, 125, 9928; d) M. L. Kantam, B. P. C. Rao, B. M. Choudary, K. K. Rao, B. Sreedhar, Y. Iwasawa, T. J. Sasaki, *J. Mol. Catal. A* **2005**, 229, 67; e) E. P. Ng, D. Chateigner, T. Bein, V. Valtchev, *Science* **2012**, 335, 70; f) M. Choi, H. S. Cho, R. Srivastava, C. Venkatesan, D. H. Choi, R. Ryoo, *Nat. Mater.* **2006**, 5, 718.
- [9] M. Choi, K. Na, R. Ryoo, *Chem. Commun.* **2009**, 2845.
- [10] a) C. T. Kresge, M. E. Leonowicz, W. J. Roth, J. C. Vartuli, J. S. Beck, *Nature* **1992**, 359, 710; b) Y. Xia, R. Mokaya, *J. Mater. Chem.* **2004**, 14, 863; c) A. Karlsson, M. Stocker, R. Schmidt, *Microporous Mesoporous Mater.* **1999**, 27, 181; d) S. P. Naik, J. C. Chen, A. S. T. Chiang, *Microporous Mesoporous Mater.* **2002**, 54, 293; e) S. P. Naik, A. S. T. Chiang, R. W. Thompson, F. C. Huang, H. M. Kao, *Microporous Mesoporous Mater.* **2003**, 60, 213; f) F. Hasan, R. Singh, G. Li, D. Zhao, P. A. Webley, *J. Colloid Interface Sci.* **2012**, 382, 1.
- [11] a) M. Choi, K. Na, J. Kim, Y. Sakamoto, O. Terasaki, R. Ryoo, *Nature* **2009**, 461, 246; b) W. Park, D. Yu, K. Na, K. E. Jelfs, B. Slater, Y. Sakamoto, R. Ryoo, *Chem. Mater.* **2011**, 23, 5131; c) K. Na, C. Jo, J. Kim, K. Cho, J. Jung, Y. Seo, R. J. Messinger, B. F. Chmelka, R. Ryoo, *Science* **2011**, 333, 328; d) J. Jung, C. Jo, K. Cho, R. Ryoo, *J. Chem. Mater.* **2012**, 22, 4637; e) W. Kim, J. C. Kim, J. Kim, Y. Seo, R. Ryoo, *ACS Catal.* **2013**, 3, 192.
- [12] L. Wu, V. Degirmenci, P. C. M. M. Magusin, B. M. Szyja, E. J. M. Hensen, *Chem. Commun.* **2012**, 48, 9492.
- [13] a) J. Kim, M. Choi, R. Ryoo, *J. Catal.* **2010**, 269, 219; b) C. C. Lin, S. W. Park Jr., W. Hatcher, *J. Ind. Eng. Chem. Process Des. Dev.* **1983**, 22, 609; c) J. W. Park, S. J. Kim, M. Seo, S. Y. Kim, Y. Sugi, G. Seo, *Appl. Catal. A* **2008**, 349, 76.
- [14] B. O. Hincapie, L. J. Garces, Q. Zhang, A. Sacco, S. L. Suib, *Microporous Mesoporous Mater.* **2004**, 67, 19.
- [15] a) A. N. C. van Laak, S. L. Sagala, J. Zecevic, H. Friedrich, P. E. de Jongh, K. P. de Jong, *J. Catal.* **2010**, 276, 170; b) X. Li, R. Prins, J. A. Bokhoven, *J. Catal.* **2009**, 262, 257.
- [16] a) Z. Tang, B. Xu, B. Wu, M. W. Germann, G. Wang, *J. Am. Chem. Soc.* **2010**, 132, 3367; b) Z. Li, R. Jin, C. A. Mirkin, R. L. Letsinger, *Nucleic Acids Res.* **2002**, 30, 1558.